Effects of sintering pressure on the densification and mechanical properties of nanosilver double side sintered power module

Zhang, Hao; Liu, Yang; Wang, Lingen; Sun, Fenglian; Fan, Jiajie; Placette, Mark D.; Fan, Xuejun; Zhang, Guoqi

DOI
10.1109/TCPMT.2018.2884032

Publication date
2019

Document Version
Accepted author manuscript

Published in
IEEE Transactions on Components, Packaging and Manufacturing Technology

This article has been accepted for publication in a future issue of this journal, but has not been fully edited. Content may change prior to final publication. Citation information: DOI 10.1109/TCPMT.2018.2884032, IEEE Transactions on Components, Packaging and Manufacturing Technology

Effects of sintering pressure on the densification and mechanical properties of nanosilver double side sintered power module

Hao Zhang, Yang Liu, Lingen Wang, Fenglian Sun, Jiajie Fan, *Senior Member, IEEE*, Mark D. Placette, Xuejun Fan, *Fellow, IEEE*, Guoqi Zhang, *Fellow, IEEE*

***Abstract*—Modern power electronics has the increased demands in current density and high temperature reliability. However, these performance factors are limited due to the die attach materials used to affix power dies microchips to electric circuitry. Although several die attach materials and methods exist, nanosilver sintering technology has received much attention in attaching power dies due to its superior high temperature reliability. This paper investigated the sintering properties of nanosilver film in double side sintered power packages. X-ray diffraction (XRD) results revealed that the size of nanosilver particles increased after pressure-free sintering. Comparing with the pressure-free sintered nanosilver particles, the 5 MPa sintered particles showed a higher density. When increasing sintering pressure from 5 to 30 MPa, the shear strength of the sintered package increased from 8.71 MPa to 86.26 MPa. When sintering at pressures below 20 MPa, the fracture areas are mainly located between the sintered Ag layer and the surface metallization layer on the fast recovery diode (FRD) die. The fracture occurs through the FRD die and the metallization layer on bottom Mo substrate when sintering at 30 MPa.**

***Index Terms*—power electronics, nanosilver sintering, shear strength, fracture**

I. Introduction

THE rapid development of wide-band gap semiconductors have facilitated power electronics becoming key components in hybrid electric vehicles, traction, wind turbine and high-voltage power transmission systems due to their combined advantages of fast switch speed and low power consumption [1-3]. Despite these promising attributes, the development trends of power electronics require increased current carrying capacity and higher operating temperatures. This proposes a challenge to power electronics' packaging components, particularly die attachment materials. The die attach layer plays an important role in power electronics. Yu *et al*. [4] indicated that the die attach layers are responsible for mechanical connection of microelectronics to the substrate, thermal dissipation of processing units, and electric conduction. Therefore, the effectiveness of the die attach layer significantly contributes to the overall performance of the entire package. Moreover, die attach materials typically limit the operating temperature and power density of the device. In the work of Navarro *et al*. [5], the silicon-based packages, for example, have an operating temperature of only about 175°C and a power density of 200 W/cm^2. These physical limitations as well as the health concerns of lead-based solders have led to alternative die attach technologies.

Currently, several advanced die attach materials and methods of attachment exist that increase electrical/temperature performance of power electronic devices, but the manufacturing and service processes often reduce mechanical reliability and manufacturing efficiency. For instance, Gold-tin eutectic solder alloy has been widely used as soldering material in attaching power dies due to its favorable mechanical properties and capability of fluxless soldering [6, 7]. Huang *et al*. [8] implied that the AuSn eutectic layer has been proven to provide good electrical and thermal conductivity, and reliable high temperature interconnection for power electronics. However, Wang *et al*. [9] proved that the coarsening of microstructure in the service process decreased the reliability of AuSn solder joint. In addition, Arabi *et al*. [10] suggested that the voids can cause localized stress and cracks under thermal cycles as well as thermal stress from its high processing temperature which limit the wide application of AuSn solder alloy. Transient liquid phase (TLP) bonding technology has been developed as a die attaching process in response to increased concerns over lead-based attachments. As described by Khazaka *et al*. [11], a metallic interlayer is usually used in the TLP process, such as Sn or In. This interlayer reacts under low pressure with a substrate that has a higher melting point, such as Cu, Ag, Ni, Au [12-15]. The formed die attach layer

The work described in the paper was partially supported by the National High Technology Research and Development Program of China (863 Program) (No. 2015AA033304), partially supported by the National Natural Science Foundation of China (No. 51604090), and partially supported by the Natural Science Foundation of Heilongjiang Province (No. E2017050). (Corresponding authors: Hao Zhang and Guoqi Zhang.)

Hao Zhang is with the EEMCS Faculty, Delft University of Technology, 2628CD, Delft, The Netherlands, and School of Materials Science and Engineering, Harbin University of Science and Technology, Harbin 150040, China (e-mail: hoayzhang@163.com).

Y. Liu and F. Sun are with the School of Materials Science and Engineering, Harbin University of Science and Technology, Harbin 150040, China.

L. Wang is with the Department of Packaging, Boschman Technologies B.V., 6921EX, Duiven, The Netherlands.

J. Fan is with the College of Mechanical and Electrical Engineering, Hohai University, Changzhou 213022, China.

Mark D. Placette is with the Department of Mechanical Engineering, Iowa State University, Ames, Iowa 50011, USA.

X. Fan is with the Department of Mechanical Engineering, Lamar University, Beaumont, TX 77710 USA.

G. Zhang is with the EEMCS Faculty, Delft University of Technology, 2628CD, Delft, The Netherlands. (e-mail: g.q.zhang@tudelft.nl).

This article has been accepted for publication in a future issue of this journal, but has not been fully edited. Content may change prior to final publication. Citation information: DOI 10.1109/TCPMT.2018.2884032, IEEE Transactions on Components, Packaging and Manufacturing Technology

consists of full intermetallic compounds (IMCs) and its remelting temperature is much higher than the melting point of the corresponding solder material. But Shao *et al*. [16] found that the TLP process is quite time consuming because of the diffusion dominated reaction between the interlayer and substrate, and IMCs are brittle causing performance issues.

Recently, nanosilver sintering technology has shown great potential in attaching power dies while potentially maintaining favorable physical properties [17]. The nanosilver particles are usually mixed with dispersant, binder and thinner to form nanosilver paste, which can be further screen printed or dispensed on the substrate. The nanosilver paste can be sintered at low temperatures around 250 ℃ to form a bonding, and then serve at relatively high temperatures. Bai *et al*. [18] reported that the electrical conductivity and thermal conductivity of pressure-free sintered Ag layer can reach as high as 2.6×10^7 /(Ω·m) and 240 W/(m·K), respectively. However, Qi *et al*. [19] indicated that low shear strength is generated in sintered Ag layer without the assistance of pressure, especially when die sizes are larger than 9 mm^2. It was reported by Ogura *et al*. [20] that the fracture surface of pressure-free sintered nanosilver layer exhibited uneven morphology with randomly distributed weak spots on the bonding area. In addition, as demonstrated by Knoerr and Schletz [21], the density of sintered Ag layer can be improved from 58% to 90% when the sintering pressure increased from 0 MPa to 30 MPa. The increased density will also be beneficial for the improvement of electrical and thermal conductivity of sintered Ag layer. Zhao *et al*. [22] have already applied pressure assisted sintering in industrial production, and the thermal shock test results revealed that the better reliability of pressure sintered power module was obtained when comparing with soldered power module. Therefore, the sintering pressure is quite necessary to ensure the long term high temperature reliability of power package, especially for bonding package with large dies.

The applied pressure during sintering increases particle density and contact between nanosilver particles, and thus achieves better mechanical, electrical, and thermal properties. During sintering, the organic shells will first evaporate and allow coalescence between particles, as shown in Fig. 1 (a). The free energy of nanosilver particles decreases by reducing the surface area. Then the sintering necks are irregularly formed between adjacent particles without pressure, as depicted in Fig. 1 (b). As demonstrated by Peng *et al*. [23], the densification rate of particles during sintering process can be expressed by equation (1):

$$\frac{d\rho}{dt}=\frac{3}{2}\sigma(1-\rho)\left(1-\alpha\left(\frac{1}{\rho}-1\right)^{\frac{1}{3}}\ln\frac{1}{1-\rho}\right)\frac{1}{\eta} \quad (1)$$

where $d\rho/dt$ represents the densification rate, σ represents the driving force for densification, α represents the geometrical constant, ρ represents the density, and η represents the densification viscosity. Mackenzie and Shuttleworth [24] used equation (2) to express the driving force σ between two particles:

$$\sigma=\gamma\left(\frac{1}{R_1}+\frac{1}{R_2}\right)+P \quad (2)$$

where γ represents the surface energy of material, R_1 and R_2 represents the principal radii of curvature at the contact point, and P represents the applied pressure. Based on the equation above, it can be concluded that the densification will be enhanced by decreasing the particle size and the increasing the applied pressure. During pressure assisted sintering process, the nanosilver particles will be compressed tighter and thus resulting in the more and larger contact surface area as seen in Fig. 1 (c) when comparing with pressure-free sintered particles. Greater number sintering necks are formed with larger contact areas, which would further enhance the bonding quality and performance of the sintered layer. A more continuous matrix of nanosilver would then be indicative of better performance properties.

According to our previous test results [25], the two Molybdenum (Mo) substrates, coated with Ag/Cu/Ni(Mo), were successfully bonded by the sintering of nanosilver film. In this paper, a real power module that involves with power dies was studied. We are trying to apply this result in our further test to verify the feasibility in bonding real products, which involves the power dies. This paper investigated the effect of sintering pressure on nanosilver films and double-sided nanosilver sintered power packages. Particle densification of the nanosilver films during fabrication can have significant effects on the performance of the package, and this effect was examined by comparing sintered, not sintered, and pressure-assisted nanosilver films. The thermal behavior of nanosilver film was studied by differential scanning calorimetry (DSC) test. The morphology and phase composition of the pure nanosilver film before and after pressure-free sintering were investigated by scanning electron microscopy (SEM) and X-ray diffraction (XRD), respectively.

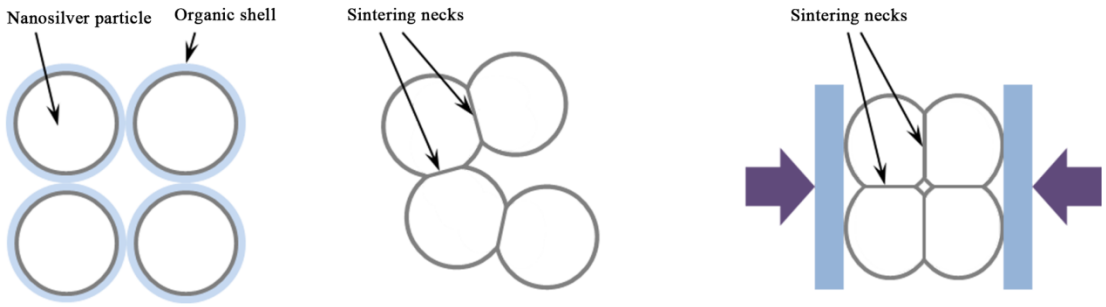

Fig. 1. Schematic diagram of sintered nanosilver particles, (a) original particles; (b) pressure-free sintered; (c) pressure assisted sintered

This article has been accepted for publication in a future issue of this journal, but has not been fully edited. Content may change prior to final publication. Citation information: DOI 10.1109/TCPMT.2018.2884032, IEEE Transactions on Components, Packaging and Manufacturing Technology

The morphologies of pressure-free and pressure-assisted sintered nanosilver film were then compared by SEM. The mechanical performance of a power package often limits its reliability. The mechanical performance of pressure sintered power packages in this paper were determined by shear tests for a variety of sintering pressures. The fracture morphologies achieved by the shear tests were then further analyzed by SEM to demonstrate the effect of sintering pressure on bonding strength. Energy-dispersive X-ray spectroscopy (EDS) was conducted in conjunction with SEM to determine material transfer after fracture.

II. Experimental Procedures

A. Nanosilver film material investigation

The nanosilver film was the commercial sintering material from Alpha Assembly. In order to characterize the structure and phase composition of sintered nanosilver particles, two pure nanosilver films were sintered at 250°C for 3 min. One film was pressure-free sintered, and another was sintered with a pressure of 5 MPa. SEM was used to investigate the morphology of nanosilver of these two samples. X-ray Diffraction (XRD) was conducted to investigate the crystal structures of the pressure-free nanosilver particles. All films in this analysis and this paper had a thickness of 65 μm. Besides, the DSC test was performed for nanosilver film in N_2 atmosphere, and the heating range and heating rate was set as 130 to 260 ℃ and 10 ℃/min, respectively.

B. Power package fabrication

Four power packages were produced for the shear tests in this study. Each power package was fabricated with novel equipment, Sinterstar Innovate-F-XL, which could precisely and uniformly control the applied pressure at high temperatures through the real time feedback system embedded in the equipment, as shown in Fig. 2. There are three main steps in fabricating these power packages as seen in Fig. 2. First, two Molybdenum (Mo) substrates were laminated with nanosilver film on one side. The Mo substrate was coated with several layers on the top and bottom surfaces: Ag/Cu/Ni/(Mo substrate). The larger Mo substrate was to be the bottom Mo substrate with dimension of 13.6×13.6×2.0 mm^3, and the smaller was to be the top Mo substrate with dimension of 9.4×9.4×1.2 mm^3. This process was achieved at 130 ℃ with the pressure of 5 MPa for 2 min. Second, the FRD die (13.53×13.53×0.41 mm^3) coated with Ag on the top surfaces of up and down sides was placed on the laminated side of the bottom Mo substrate, and then sintered at 250 ℃ for 3 min. In order to investigate the effects of sintering pressure on the bonding quality of the sintered Ag layer, four samples were created, each at different applied pressures of 5, 10, 20, 30 MPa during the sintering process in this step. Then, the laminated side of the top Mo substrate was placed on the top of the sintered bottom Mo substrate. The assembled package was then sintered at 250 ℃ for 3 min and the same sintering pressure was used as last step. The entire process was achieved in air. The schematic diagram of cross section of double side sintered power package is shown in Fig. 2, and the thickness of each layer is also marked.

C. Shear and fracture tests of power packages

To determine the mechanical properties of sintered Ag layer, a shear test was performed on the Instron 5569 electromechanical test machine. The test settings were based on the standard of MIL-STD-883E, Method 2019.5. The sintered package was first secured in a special designed rigid frame and a constant test speed was set as constant of 0.3 mm/min, as shown in Fig. 3. The mechanical properties of sintered package were measured in displacement control mode. The fracture surface morphology of sheared sample was examined by SEM and EDS.

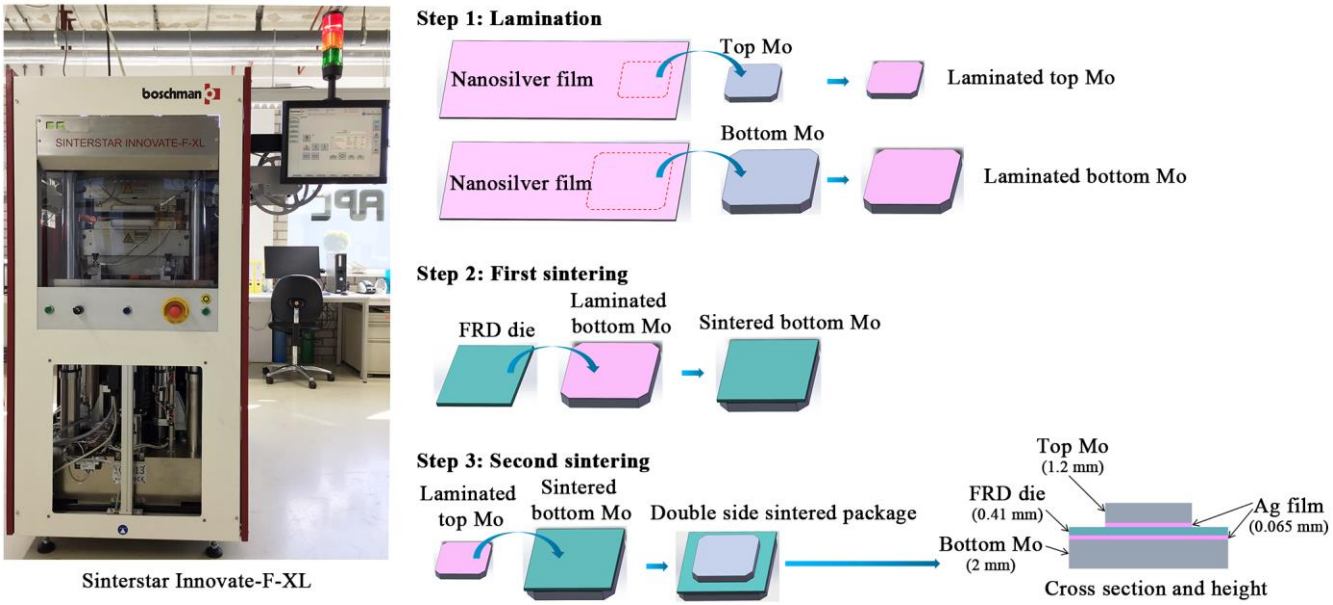

Fig. 2. Sintering equipment and schematic diagram of fabrication process (not drawn to scale)

This article has been accepted for publication in a future issue of this journal, but has not been fully edited. Content may change prior to final publication. Citation information: DOI 10.1109/TCPMT.2018.2884032, IEEE Transactions on Components, Packaging and Manufacturing Technology

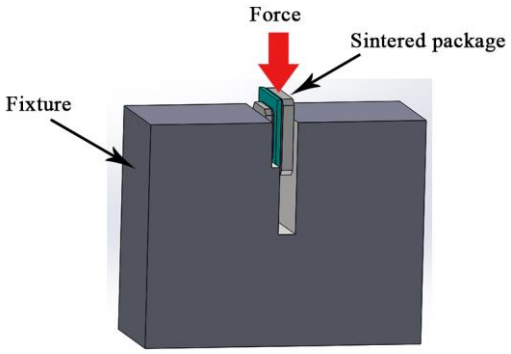

Fig. 3. Schematic diagram of the shear test

III. Results

A. Characterization of pressure-free sintered nanosilver film

The thermal behavior of nanosilver film is first investigated by DSC test. Fig. 4 shows the DSC heat curve of nanosilver film within the temperature range of 130-260 ℃. As indicates in the figure, one exothermic peak at approximately 220-240 ℃ is obviously observed during heating process. When the sintering temperature increases to 220 ℃, the organics inside the nanosilver film decompose gradually. It is suggested that the coalescence of silver nanoparticles starts at this temperature. The decomposition of organics ends around 240 ℃. Therefore, it is reasonable to conclude that the sintering temperature of nanosilver film should be higher than 240 ℃ in order to get the good bonding between silver nanoparticles. In this paper, the temperature of 250 ℃ is selected for the sintering tests.

An initial SEM investigation was conducted to examine morphologies of pure nanosilver film before and after sintering, as shown in Fig. 5 (a) and 5 (b) respectively. The nanosilver particles are coated with a nearly transparent layer on the surface, which can prohibit the aggregation between particles, as shown in Fig. 5 (a). The nanosilver particles have an average diameter around 200 nm. The close contact of nanosilver particles is likely to result from the compression during the film fabrication process. During sintering, the organic shells start to decompose and allow adjacent nanosilver particles to combine with each other. This combining of particles is seen upon comparing Fig. 5 (a) and 5 (b). Li *et al*. [26] suggested that surface diffusion is the primary sintering mechanism at the beginning of the sintering process due to its lowest activation energy, and then followed by grain boundary diffusion and lattice diffusion as temperature increases. After pressure-free sintering at 250°C for 3 min, sintering necks are formed between particles, which indicate bonding of the nanosilver layer, as shown in Fig. 5 (b).

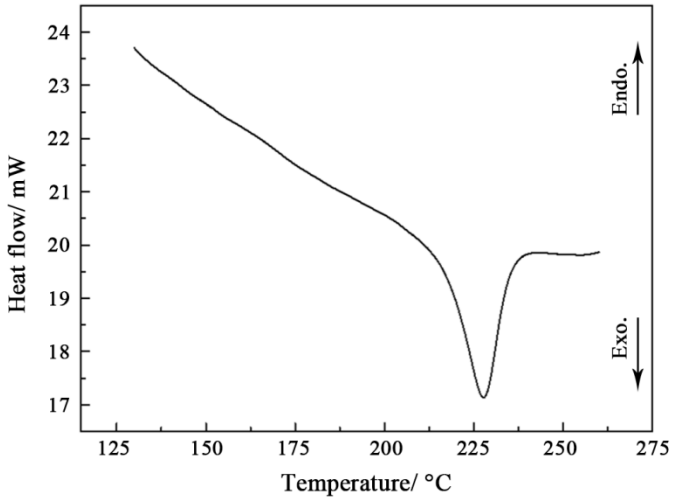

Fig. 4. DSC heat curve of nanosilver film

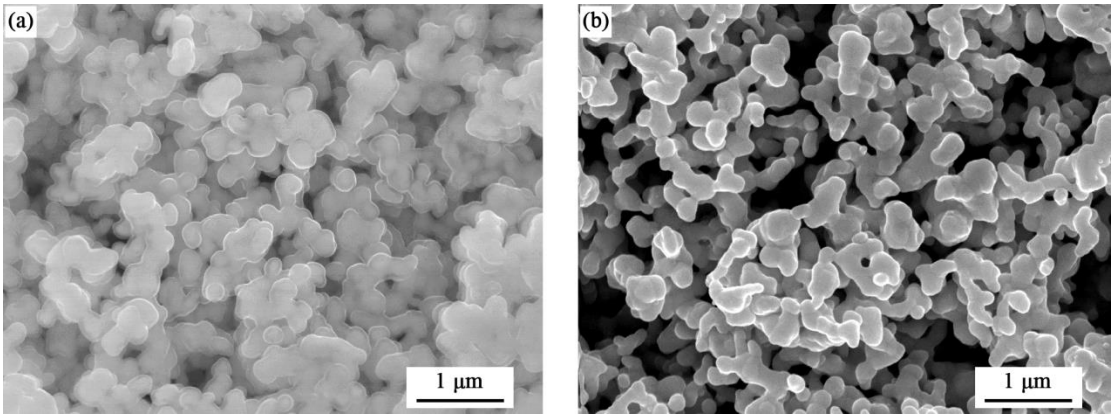

Fig. 5. SEM images of nanosilver film, (a) original; (b) pressure-free sintered at 250°C for 3 min

Crystal structures of nanosilver particles before and after pressure-free sintering at 250°C for 3 min were studied with XRD, and the results are shown in Fig. 6. According to the test results, five obvious peaks appear in the original nanosilver film, and the corresponding crystal plane index is (111), (200), (220), (311) and (222), respectively. Because of the existence of a large number of oriented small crystal particles in the irradiated area, the nanosilver particles exhibit a polycrystalline structure. The full width at half maximum (FWHM) of the nanosilver particles are listed in Table 1 for the crystal planes found in Fig. 6. Comparing the FWHM of nanosilver particles before and after sintering, the peaks of sintered particles show slightly narrowed width due to the increased particle size. Similar results have been obtained by sintering different types of silver particles [27, 28]. In addition, there is no oxidation peak observed after sintering in air. This result indicates that the

This article has been accepted for publication in a future issue of this journal, but has not been fully edited. Content may change prior to final publication. Citation information: DOI 10.1109/TCPMT.2018.2884032, IEEE Transactions on Components, Packaging and Manufacturing Technology

nanosilver particles are not greatly oxidized and the formed sintered joint is mainly composed of silver particles, which also implies good bonding between nanosilver particles.

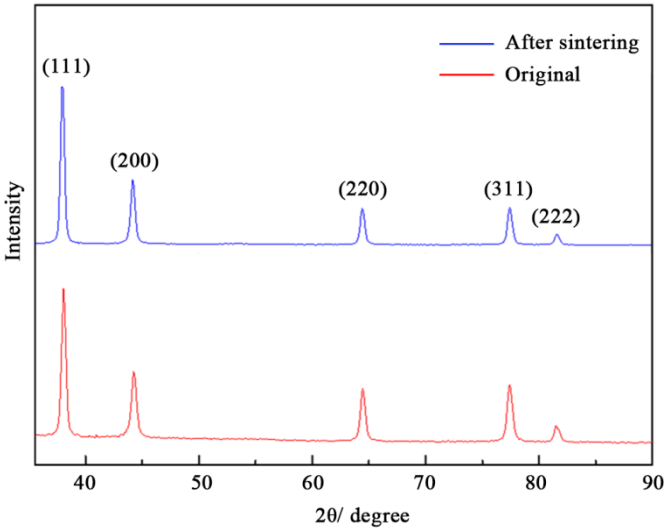

Fig. 6. XRD spectra of nanosilver particles before and after sintering

B. Comparison of pressure-free and pressure-assisted sintering nanosilver particles

An SEM study was conducted to investigate the effect of applied pressure during sintering on the structure of nanosilver particles. The results in Fig. 7 (a) and 7 (b) show the pressure-free and 5 MPa sintered layers respectively. As seen in Fig. 7 (a), the overall morphology of pressure-free sintered nanosilver particles shows an irregular structure. Some of the particles only combine with the nearest ones, which will result in the discontinuous matrix. However, the dense and well-structured sintered Ag layer seen in Fig. 7 (b) is achieved with the help of sintering pressure. Most of the particles have formed sintering necks with particles around them. Comparing the micrographs also illustrates that the pressure-free sintered structure is more porous. The porosity of pressure-free and 5 MPa sintered nanosilver particles were measured using Image-J software and the corresponding result is 16.26% and 5.38%, respectively. These results and the results in the previous section confirm both sintering and pressure during nanosilver sintering may enhance the performance of the power package.

TABLE I FWHM OF NANOSILVER PARTICLES

Nanosilver particles	2θ/ degree (111)	2θ/ degree (200)	2θ/ degree (220)	2θ/ degree (311)	2θ/ degree (222)
Original	0.46	0.54	0.52	0.56	0.60
After sintering	0.41	0.46	0.47	0.50	0.50

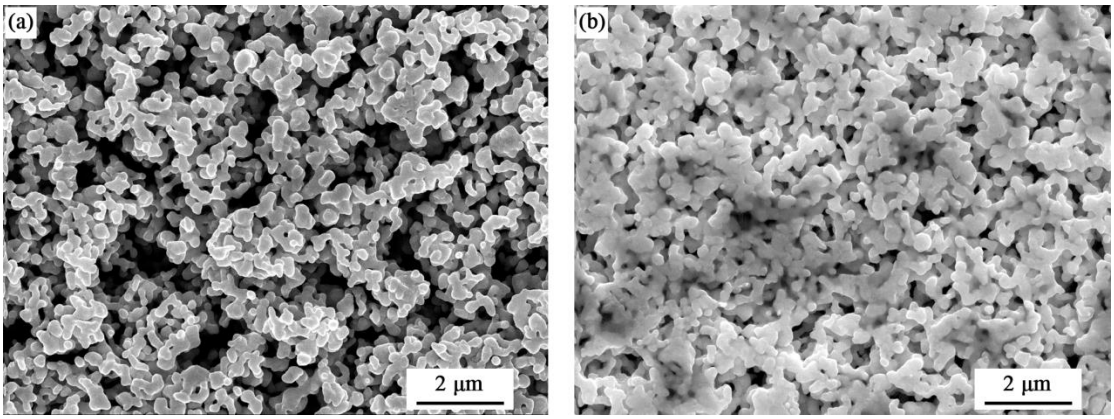

Fig. 7. Comparison of sintered nanosilver particles at 250 ℃ for 3 min, (a) 0 MPa, (b) 5 MPa

C. Mechanical properties of sintered package

During sintering, the formation of necks between particles can be enhanced with the help of applied pressure and finally result in the high mechanical properties. The shear strength of sintered package reveals an increasing trend with the increase of sintering pressure, as shown in Fig. 8. The average shear strength of 5 MPa sintered package is 8.71 MPa. When sintering pressure increases to 10 MPa, the sintered package has the average shear strength of 24.68 MPa and the increase rate is 64.71%. The maximum increase rate of 65.83% is achieved when pressure increases from 10 MPa to 20 MPa. The highest shear strength of 86.26 MPa is obtained at a pressure of 30 MPa. This gives empirical evidence that pressure-assisted sintering will increase the mechanical performance of the package, but the rate of increase is most effective between 10 and 20 MPa.

D. Fracture surface morphology analysis of sintered package

Shear tests were conducted on the power packages, and the fracture morphologies of a sintered package under 5 MPa are shown in Fig. 9. According to the optical image in Fig. 9 (a), the fracture area is mainly located at the interface between the sintered Ag layer and the surface metallization layer on FRD die. The top Mo substrate and the whole sintered Ag layer are peeled off the package, which indicates weak bonding between sintered nanosilver particles and die surface metallization. The fracture surface of sintered Ag layer is quite smooth, as shown in the partial magnified image in Fig. 9 (b) and (c). The detailed morphology is shown in Fig. 9 (d), and there are only sintered

This article has been accepted for publication in a future issue of this journal, but has not been fully edited. Content may change prior to final publication. Citation information: DOI 10.1109/TCPMT.2018.2884032, IEEE Transactions on Components, Packaging and Manufacturing Technology

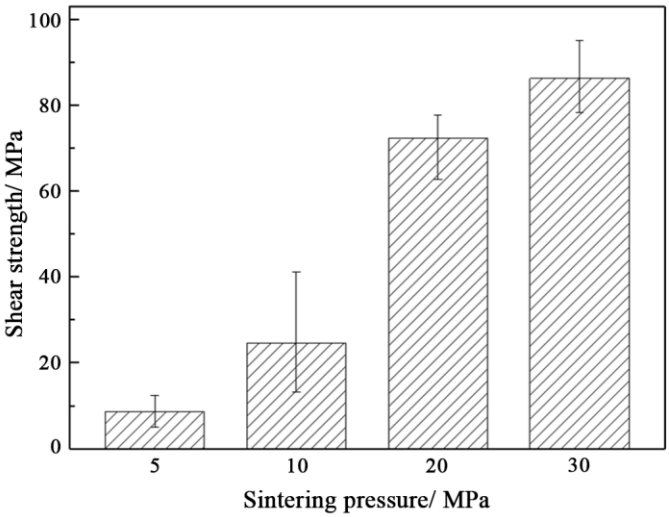

Fig. 8. Relationship between sintering pressure and shear strength

nanosilver particles found in this location, which can be identified by energy-dispersive X-ray spectroscopy (EDS) in Fig. 9 (e). In addition, the fracture surface in Fig. 9 (d) is not flat and pores with various sizes are formed between particles.

Fig. 10 displays the fracture morphology of 10 MPa sintered package. Similar to the 5 MPa sintered package, the facture area in this package is also located at the interface between the sintered Ag layer and the surface metallization layer on FRD die, as shown in Fig. 10 (a). The magnified fracture morphologies are quite flat and smooth, as seen in Fig. 10 (b) and (c), which indicates the uniform diffusion bonding of nanosilver particles under 10 MPa pressure. Based on the magnified image in Fig. 10 (d) and the EDS analysis in Fig. 10 (e), the fracture surface mainly consists of sintered nanosilver particles. The sintered nanosilver particles have a lower porosity when comparing with the 5 MPa sintered ones in Fig. 10 (d).

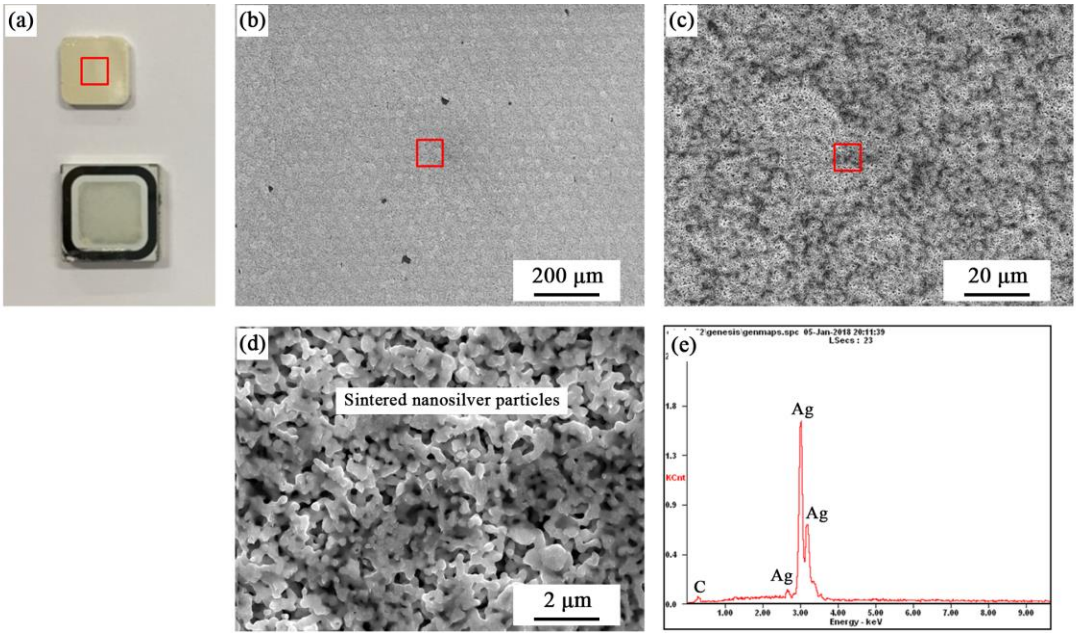

Fig. 9. Fracture morphology of sintered package under 5 MPa, (a) optical image of fracture surface; (b), (c) and (d) are the gradually partial magnified image of (a); (e) EDS pattern of the fracture surface in (d)

However, as the sintering pressure increases to 20 MPa, the fracture occurs partially on the FRD die and partially on the sintered Ag layer, as shown in Fig. 11 (a). The sintering pressure of 20 MPa has an obvious effect of strengthening the bonding between sintered Ag layer and metallization layer on FRD die. As seen in Fig. 11 (b) and its magnified image in Fig. 11 (c), the fracture surface is not flat and there are many depressions on it. More details can be obtained from Fig. 11 (d), the fracture area is composed of Ag coating on FRD die and the sintered Ag particles. The element composition is proven by EDS results in Fig. 11 (e), showing no significant material transfer other than the sintered silver.

At 30 MPa, fracture occurs through the FRD die and the metallization layer on bottom Mo substrate as shown in Fig. 12 (a). The fracture surface of 30 MPa sintered package is quite rough, which is different from other packages that are sintered at pressures lower than 30 MPa, as shown in Fig. 12 (b). The further magnified image is shown in Fig. 12 (c), and the fracture surface is partially lifted up and partially ripped. More details are depicted in Fig. 12 (d), and no nanosilver particles are found on the surface. According to the EDS analysis in Fig. 12 (e), the facture area is located at the metallization layer on the Mo substrate, which contains Ag, Cu and Ni elements.

Combining the results of Fig. 8 and Figures 9-12, there is strong evidence that increasing the applied pressure when sintering increases the shear and bonding strength of the package, but only at pressures below 30 MPa. The change of fracture area may due to the enhanced bonding strength of metallization layer under high sintering pressures. Dudek *et al.* [29] also proved that the bonding quality of metallization layer can be improved by the increased sintering pressure from 5 MPa to 20 MPa, which resulted in the change of fracture area

This article has been accepted for publication in a future issue of this journal, but has not been fully edited. Content may change prior to final publication. Citation information: DOI 10.1109/TCPMT.2018.2884032, IEEE Transactions on Components, Packaging and Manufacturing Technology

from the die attach layer to the die. Based on the results above, it can be concluded that a sintering pressure higher than 5 MPa is quite useful to ensure the high bonding quality of sintered package. However, the sintering pressure beyond 20 MPa may not be optimal for manufacturing due to the limited increase rate in shear strength when increasing the sintering pressure from 20 MPa to 30 MPa.

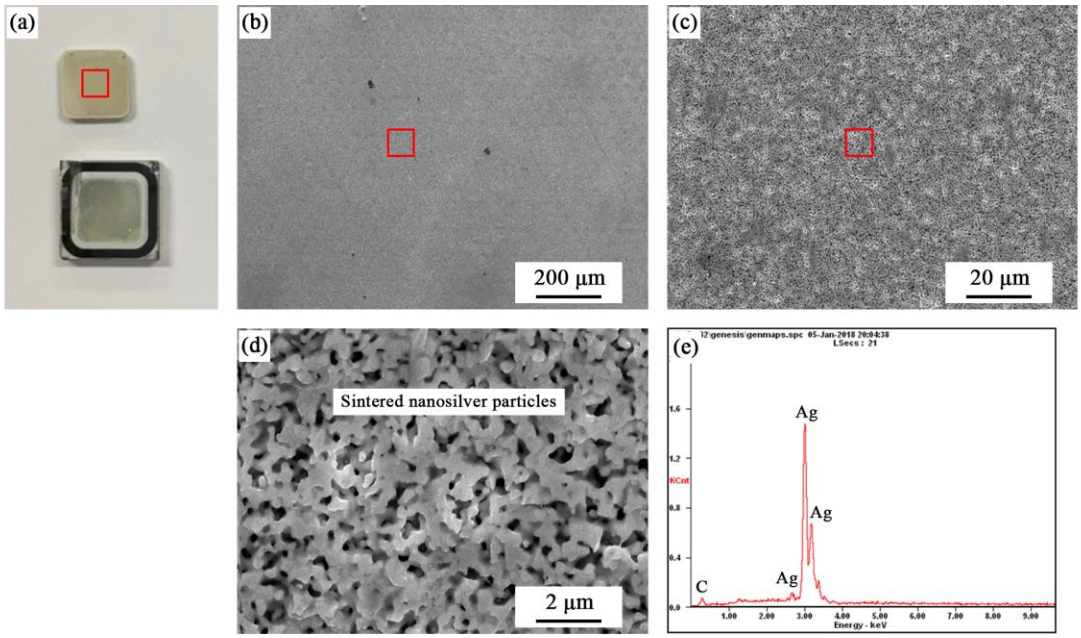

Fig. 10. Fracture morphology of sintered package under 10 MPa, (a) optical image of fracture surface; (b), (c) and (d) are the gradually partial magnified image of (a); (e) EDS pattern of the fracture surface

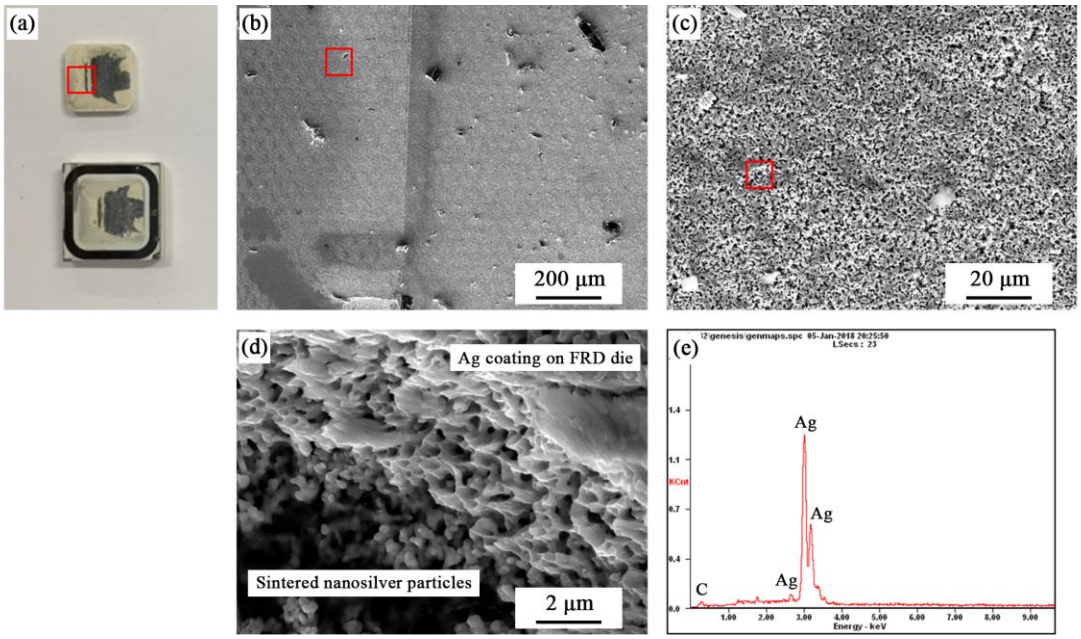

Fig. 11. Fracture morphology of sintered package under 20 MPa, (a) optical image of fracture surface; (b), (c) and (d) are the gradually partial magnified image of (a); (e) EDS pattern of the fracture surface

IV. Conclusions

According to the crystal structure analysis before and after pressure-free sintering, the peaks of sintered particles exhibit slight narrowed width due to the increased particle size. The overall morphology of pressure-free sintered nanosilver particles shows irregular and discontinuous matrix. However, a dense and well-structured sintered layer was obtained with the help of 5 MPa sintering pressure. This result indicates that the application of sintering pressure during nanosilver sintering may enhance the performance of the power package. The shear strength of sintered package increases with pressure increasing from 5 MPa to 30 MPa. The highest increase rate was obtained when sintering pressure increases from 10 to 20 MPa. The fracture areas are mainly locate between the sintered Ag layer and the surface metallization layer on FRD die at sintering

This article has been accepted for publication in a future issue of this journal, but has not been fully edited. Content may change prior to final publication. Citation information: DOI 10.1109/TCPMT.2018.2884032, IEEE Transactions on Components, Packaging and Manufacturing Technology

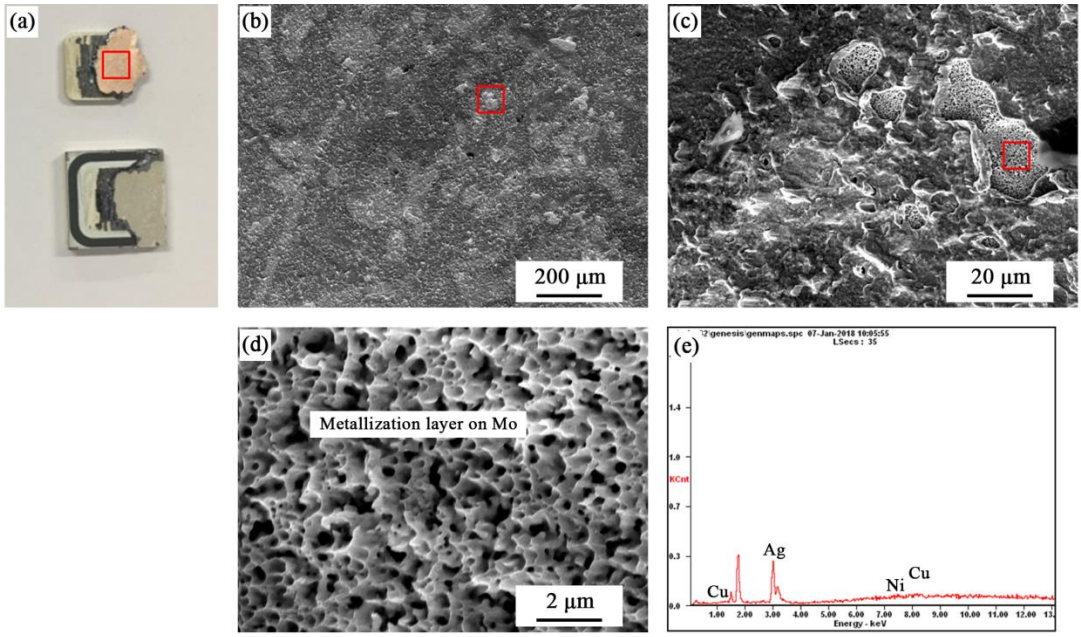

Fig. 12. Fracture morphology of sintered package under 30 MPa, (a) optical image of fracture surface; (b), (c) and (d) are the gradually partial magnified image of (a); (e) EDS pattern of the fracture surface

pressures lower than 20 MPa, and finally change to the FRD die and even the metallization layer on bottom of Mo at 30 MPa. However, the shear tests indicate increasing the sintering pressure beyond 20 MPa may not be optimal for manufacturing.

REFERENCES

[1] X. She, A. Q. Huang, Ó. Lucía, and B. Ozpineci, "Review of Silicon Carbide Power Devices and Their Applications," *IEEE T. Ind. Electron.*, vol. 64, pp. 8, pp. 193-8205, Oct. 2017.

[2] J. Li, C. M. Johnson, C. Buttay, W. Sabbah, and S. Azzopardi, "Bonding strength of multiple SiC die attachment prepared by sintering of Ag nanoparticles," *J. Mater. Process. Tech.*, vol. 215, pp. 299-308, Jan. 2015.

[3] S. A. Paknejad and S. H. Mannan, "Review of silver nanoparticle based die attach materials for high power/temperature applications," *Microelectron. Reliab.*, vol. 70, pp. 1-11, Mar. 2017.

[4] F. Yu, J. Cui, Z. Zhou, K. Fang, R. W. Johnson, and M. C. Hamilton, "Reliability of Ag Sintering for Power Semiconductor Die Attach in High-Temperature Applications," *IEEE T. Power Electr.*, vol. 32, no. 9, pp. 7083-7095, Sept. 2017.

[5] L. A. Navarro, X. Perpiñà, P. Godignon, J. Montserrat, V. Banu, M. Vellvehi, and X. Jordà, "Thermomechanical Assessment of Die-Attach Materials for Wide Bandgap Semiconductor Devices and Harsh Environment Applications," *IEEE T. Power Electr.*, vol. 29, no. 5, pp. 2261-2271, May 2014.

[6] J. W. Yoon, H. S. Chun, and S. B. Jung, "Reliability evaluation of Au–20Sn flip chip solder bump fabricated by sequential electroplating method with Sn and Au," *Mat. Sci. Eng. A-Struct.*, vol. 473, no. 1-2, pp. 119-125, Jan. 2008.

[7] H. Zhang, J. Fan, J. Zhang, C. Qian, X. Fan, F. Sun, and G. Zhang, "Reliability optimization of gold-tin eutectic die attach layer in HEMT package," *SSLChina*, Beijing, China, 2016, pp. 52-56.

[8] Y. Huang, W. Liu, Y. Ma, Y. Wang, and S. Tang, "Effects of cooling rate and magnetic field on solidification characteristics of Au80Sn20 eutectic solder," *J. Mater. Sci. Mater. Electron.*, vol. 29, no. 1, pp. 436-445, Jan. 2018.

[9] Y. Wang, W. Liu, Y. Ma, Y. Huang, Y. Tang, F. Cheng, and Q. Yu, "Indentation size effect and micromechanics characterization of intermetallic compounds in the Au–Sn system," *Mat. Sci. Eng. A-Struct.*, vol. 610, pp. 161-170, Jul. 2014.

[10] F. Arabi, L. Theolier, D. Martineau, J. Y. Deletage, M. Medina, and E. Woirgard, "Power electronic assemblies: Thermo-mechanical degradations of gold-tin solder for attaching devices," *Microelectron. Reliab.*, vol. 64, pp. 409-414, Sept. 2016.

[11] R. Khazaka, L. Mendizabal, D. Henry, and R. Hanna, "Survey of high-temperature reliability of power electronics packaging components," *IEEE T. Power Electr.*, vol. 30, no. 5, pp. 2456-2464, May 2015.

[12] J. Liu, H. Zhao, Z. Li, X. Song, Y. Zhao, H. Niu, H. Tian, H. Dong, and J. Feng, "Microstructure evolution, grain morphology variation and mechanical property change of Cu-Sn intermetallic joints subjected to high-temperature aging," *Mater. Charact.*, vol. 135, pp. 238-244, Jan. 2017.

[13] H. Shao, A. Wu, Y. Bao, Y. Zhao, and G. Zou, "Microstructure characterization and mechanical behavior for Ag_3Sn joint produced by foil-based TLP bonding in air atmosphere," *Mat. Sci. Eng. A-Struct.*, vol. 680, pp. 221-231, Jan. 2017.

[14] S. W. Yoon, M. D. Glover, and K. Shiozaki, "Nickel–tin transient liquid phase bonding toward high-temperature operational power electronics in electrified vehicles," *IEEE T. Power Electr.*, vol. 28, no. 5, pp. 2448-2456, May 2013.

[15] T. A. Tollefsen, A. Larsson, O. M. Løvvik, and K. E. Aasmundtveit, "High temperature interconnect and die attach technology: Au–Sn SLID bonding," *IEEE T. Comp. Pack. Man.*, vol. 3, no. 6, pp. 904-914, Jun. 2013.

[16] H. Shao, A. Wu, Y. Bao, Y. Zhao, L. Liu, and G. Zou, "Rapid Ag/Sn/Ag transient liquid phase bonding for high-temperature power devices packaging by the assistance of ultrasound," *Ultrason. Sonochem.*, vol. 37, pp. 561-570, Jul. 2017.

[17] H. Zhang, Y. Liu, L. Wang, J. Fan, X. Fan, F. Sun, and G. Zhang, " A new hermetic sealing method for ceramic package using nanosilver sintering technology," *Microelectron. Reliab.*, vol. 81, pp. 143-149, Feb. 2018.

[18] J. G. Bai, Z. Z. Zhang, J. N. Calata, and G. Q. Lu, "Low-temperature sintered nanoscale silver as a novel semiconductor device-metallized substrate interconnect material," *IEEE T. Compon. Pack. T.*, vol. 29, no. 3, pp. 589-593, Sept. 2006.

[19] K. Qi, X. Chen, and G. Q. Lu, "Effect of interconnection area on shear strength of sintered joint with nano-silver paste," *Solder. Surf. Mt. Tech.*, vol. 20, no. 1, pp. 8-12, 2008.

[20] H. Ogura, M. Maruyama, R. Matsubayashi, T. Ogawa, S. Nakamura, T. Komatsu, H. Nagasawa, A. Ichimura, and S. Isoda, "Carboxylate-Passivated Silver Nanoparticles and Their Application to Sintered Interconnection: A Replacement for High Temperature Lead-Rich Solders," *J. Electron. Mater.*, vol. 39, no. 8, pp. 1233-1240, Aug. 2010.

[21] M. Knoerr and A. Schletz, "Power semiconductor joining through sintering of silver nanoparticles: Evaluation of influence of parameters time, temperature and pressure on density, strength and reliability," *CIPS*, Nuremberg, Germany, 2010, pp. 10.3.

[22] Y. Zhao, P. Mumby-Croft, S. Jones, A. Dai, Z. Dou, Y. Wang, and F. Qin, "Silver sintering die attach process for IGBT power module production," *APEC*, Tampa, FL, USA, 2017, pp. 3091-3094.
[23] P. Peng, A. Hu, A. P. Gerlich, G. Zou, L. Liu, and Y. N. Zhou, "Joining of Silver Nanomaterials at Low Temperatures: Processes, Properties, and Applications," *Acs Appl. Mater. Interfaces*, vol. 7, no. 23, pp. 12597-12618, May 2015.
[24] J. Mackenzie and R. Shuttleworth, "A phenomenological theory of sintering," *Proc. Phys. Soc. B*, vol. 62, pp. 833-852, 1949.
[25] Y. Liu, H. Zhang, L. Wang, X. Fan, G. Zhang, and F. Sun, "Effect of sintering pressure on the porosity and the shear strength of the pressure-assisted silver sintering bonding," *IEEE T. Device Mat. Re.*, vol. 18, no. 2, pp. 240-246, Jun. 2018.
[26] J. Li, X. Li, L. Wang, Y. H. Mei, and G. Q. Lu, "A novel multiscale silver paste for die bonding on bare copper by low-temperature pressure-free sintering in air," *Mater. Design*, vol. 140, pp. 64-72, Feb. 2017.
[27] R. Zhang, K.S. Moon, W. Lin, and C. P. Wong, "Preparation of highly conductive polymer nanocomposites by low temperature sintering of silver nanoparticles," *J. Mater. Chem.*, vol. 20, pp. 2018-2023, Jan. 2010.
[28] J. H. Jeong and T. S. Cho, "Sintering Behaviors of Ag Nanopowders with Different Particle Sizes: A Real-Time Synchrotron X-ray Scattering Study," *J. Nanosci. Nanotechno.*, vol. 17, no. 10, pp. 7799-7803, Oct. 2017.
[29] R. Dudek, R. Döring, P. Sommer, B. Seiler, K. Kreyssig, H. Walter, M. Becker, and M. Günther, "Combined experimental-and FE-studies on sinter-Ag behaviour and effects on IGBT-module reliability," *EuroSime*, Ghent, Belgium, 2014, pp. 1-9.

Hao Zhang received his B.S. degree and M.S. degree from Harbin University of Science and Technology in 2013 and in 2015 respectively. Now he is pursuing his PhD degree at Delft University of Technology in Microelectronics.
His main research interests include the modification of lead free solders for microelectronic packaging, die-attach materials for power semiconductor packaging, as well as the reliability assessment and failure mechanism analysis of electronic components. He has worked in Boschman Technologies since July 2016, and mainly focuses on the sintering and molding process of power devices.

Yang Liu received the B.S. degree in materials chemistry from Lanzhou University, Lanzhou, China, in 2007, and the M.S. degree in materials processing engineering and the Ph.D. degree in materials science from the Harbin University of Science and Technology, Harbin, China, in 2010 and 2012, respectively. He is currently a Lecturer with the Department of Materials Science and Engineering, Harbin University of Science and Technology. Now he works as a guest researcher in Delft University of Technology, Delft, the Netherlands. His current research interests include LED packaging, lead-free solder materials and power electronics packaging.

Lingen Wang received the Ph.D. degree from the Delft University of Technology in 2008. He is currently the Manager of the Technical Developing Department, Boschman Technologies B.V., The Netherlands. He has rich experiences on the product and process development for advanced electronic packaging. His current developing fields include the sintering and molding for high-power electronics, packaging for MEMS and sensors, and 3-D integration packaging.

Fenglian Sun received the B.S. and Ph.D. degrees in welding engineering and materials processing engineering from the Harbin Institute of Technology, Harbin, China. She is currently the Principal Academic Leader and Ph.D. Supervisor of Materials Processing Engineering with the School of Materials Science and Engineering, Harbin University of Science and Technology, Harbin. Prof. Sun is one of the Directors of the Material Branch of the Chinese Society for Stereology, a Board Member of the Brazing and Special Welding Branch of the China Welding Association, and a Board Member of Higher Education of the Mechanical and Electronic Branch Board of the Association of Mechanical Engineering Education. As the Principal Leader, she undertook 10 projects supported by the National Natural Science Foundation of China, the State Key Laboratory Foundation, the main project of the Natural Science Foundation of Heilongjiang Province, and the Science and Technology Bureau of Harbin.

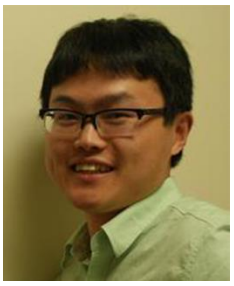

Jiajie Fan (M'14-SM'17) received the B.S. degree in Inorganic Materials Science and Engineering from Nanjing University of Technology, Nanjing, China, in 2006, the M.S. degree in Material Science and Engineering from the East China University of Science and Technology, Shanghai, China, in 2009 and the Ph.D. degree in Industrial and Systems Engineering at The Hong Kong Polytechnic University, Hung Hom, Hong Kong, China, in 2014.
Now, he is an associate professor of College of Mechanical and Electrical Engineering, Hohai University, Changzhou, Jiangsu, China. He is also working as a postdoctoral research fellow in the Delft University of Technology (Beijing Research Centre) and the State Key Laboratory of Solid State Lighting, China. He is a IEEE senior member and a register of certified Six Sigma Green Belt in Hong Kong Society for Quality (HKSQ). His main research interests include lifetime estimation for LEDs, failure diagnosis and prognosis for electric devices and system, prognostics and health management for LED lightings, and advanced electronic packaging and assembly, etc.

Mark D. Placette received his B.S. in Mechanical Engineering from Lamar University in 2011. He obtained his PhD in Mechanical Engineering from Iowa State University in 2018.
He has research interests which include high performance polymers in tribology applications, computational modeling of contact mechanics, and microelectronics reliability.

Xuejun Fan (SM'06) received the B.S. and M.S. degree in Applied Mechanics from Tianjin University, Tianjin, China, in 1984 and 1986, respectively, and the Ph.D. degree in Solid Mechanics from Tsinghua University, Beijing, China, in 1989.
He is a Professor in the Department of Mechanical Engineering at Lamar University, Beaumont, Texas, and also a visiting professor with State Key Lab of Solid State Lighting in China. His current research interests lie in the areas of design, modeling, material characterization, and reliability in heterogeneous electronic systems. He was a Senior Staff Engineer at Intel Cooperation, Chandler, Arizona, from 2004 to 2007, a Senior Member Research Staff with Philips Research Lab at Briarcliff Manor, New York from 2001 to 2004, and a Member Technical Staff and Group Leader at the Institute of Microelectronics (IME), Singapore from 1997 to 2000. In his earlier career, he was promoted to a full professor at age 27 in 1991 at Taiyuan University of Technology, Shanxi, China, and became one of the youngest full professors in China that time.
He has published over 200 technical papers, many book chapters, and three books, and several patents. Dr. Fan received IEEE Components Packaging and Manufacturing Technology (CPMT) Society Exceptional Technical Achievement Award in 2011, and won the Best Paper Award of IEEE Transactions on Components and Packaging Technologies in 2009. He is an IEEE CPMT Distinguished Lecturer.

This article has been accepted for publication in a future issue of this journal, but has not been fully edited. Content may change prior to final publication. Citation information: DOI 10.1109/TCPMT.2018.2884032, IEEE Transactions on Components, Packaging and Manufacturing Technology

Guoqi Zhang (M'03–F'14) received the Ph.D. degree in aerospace engineering from Delft University of Technology, Delft, The Netherlands, in 1993.

Since 2013, he has been a Chair Professor with the Department of Microelectronics, Delft University of Technology. He had been with Philips for 20 years as Principal Scientist (1994–1996), Technology Domain Manager (1996–2005), Senior Director of Technology Strategy (2005–2009), and Philips Fellow (2009–2013). He also had part time appointments as a Professor at the Technical University of Eindhoven (2002–2005), and as a Chair Professor at Delft University of Technology (2005–2013). He is one of the pioneers in developing the "More than Moore" (MtM) strategy when he served as a Chair of MtM Technology team of European's Nanoelectronics Platform in 2005. He has published more than 400 papers including more than 150 journal papers, 3 books, 17 book chapters, and more than 100 patents. His research interests include heterogeneous micro/nanoelectronics packaging, system integration, and reliability.

Prof. Zhang received the "Outstanding Contributions to Reliability Research" Award from the European Center for Micro/Nanoreliability, in 2007, the "Excellent Leadership Award" at EuroSimE, "Special Achievement Award" at ICEPT, and the IEEE Components, Packaging, and Manufacturing Technology Society Outstanding Sustained Technical Contribution Award in 2015.